Ibn Al-Haitham Journal for Pure and Applied Sciences
Journal homepage: jih.uobaghdad.edu.iq
PISSN: 1609-4042, EISSN: 2521-3407
IHJPAS. 2026; 39(4)

Structural, Characterization, Biological, and Studying the Enzyme Activity of Some Transition Metal Complexes with (Z)-N'-(4-Hydroxy-3,5-Dimethoxybenzylidene) Isonicotinohydrazide

Ban K. Fadil[1*], and Shaymaa H. Naji[2]
[1,2]Department of Chemistry, College of Education for Pure Science (Ibn Al-Haitham), University of Baghdad, Baghdad, Iraq
*Corresponding author

Received: 15/February/2026
Accepted: 22/June/2026
Published: 20/October/2026
https://doi.org/10.30526/39.4.4463

© 2026. The Author (s). Published by College of Education for Pure Science (Ibn Al-Haitham), University of Baghdad. This is an open-access article distributed under the terms of the Creative Commons Attribution 4.0 International License

Abstract

The new Schiff base ligand N'-(4-hydroxy-3,5-dimethoxybenzylidene) isonicotinohydrazide (L´) has been prepared through the condensation of isonicotinohydrazide in combination with 4-hydroxy-3,5-dimethoxybenzaldehyde and identified via FT-IR, UV-Vis spectroscopy, ^{1}H and ^{13}C NMR spectra, and microanalysis (CHN). Furthermore, four metal complexes, including cobalt (II), nickel (II), and palladium (II) ions, have also been synthesized and characterized using FT-IR, UV-Vis spectroscopy, magnetic susceptibility, molar conductivity measurement, and chloride content. These studies show that the molar ratio [L:M] was [2:1] for all complexes. The cobalt (II) and nickel (II) complexes had an octahedral geometry coordinated by the ligand (O, N) in a bidentate mode, whereas Cu (II) and Pd (II) had a square planar geometry. The activity of the enzyme for the ligand (L´) and its complexes via the esterase AST was additionally examined. The enzyme activity study showed that the ligand's metal complexes exhibited diverse inhibition behaviors. The prepared (L´) ligand and its metal complexes were tested against the fungus *Candida albicans* and microorganisms, including G+ bacteria (*Staphylococcus aureus* and *Enterococcus spp*.) and G- bacteria (*E. coli and Pseudomonas aeruginosa*). $[Pd(L´)_2]Cl_2$ showed good antibacterial activity against *Candida albicans*, *E. coli*, and *Pseudomonas aeruginosa*.

Keywords: Dimethoxybenzylidene, Enzyme activity, Isonicotinohydrazide, Schiff bases complexes, Transition metal complexes.

1. Introduction

The designation "Schiff bases" originally pertained to organic compounds containing the active functional group azomethine (>C=N-). These compounds were originally synthesized by the chemist Hugo Schiff via a straightforward condensation reaction involving aldehydes or ketones and primary amines[1]. They could coordinate via metal ions through the nitrogen of the imine or an atom of another group usually linked to the aldehyde[2]. Schiff bases represent a highly promising class of targets owing to their extensive array of biological activities, including antifungal, antibacterial[3], antimalarial[4], antileishmanial, anti-inflammatory, antiviral, antipyretic characteristics, and anti-cancer properties[5]. Coordination chemistry has increasingly employed Schiff bases in recent years. Comprehensive research has been undertaken on the formation of Schiff base complexes with metals, owing to the promising properties of these complexes and their wide range of applications across diverse scientific fields[6,7]. Recently, these complexes have facilitated the exploration and identification of various metal complexes[8]. Schiff base formation is widespread because of its simple synthesis, high yield, and ease of separation[9]. Schiff base complexes have extensive applications in biology, serving as antidepressants, antimicrobials, antitumor agents, anti-inflammatory agents, and other medicinal compounds.

Additionally, these complexes exhibit significant catalytic activity in numerous reactions[10]. In the present work, (Z)-N'-(4-hydroxy-3,5-dimethoxybenzylidene) isonicotinohydrazide with the complexes of [Co (II), Ni (II), Cu (II), and Pd (II)] was synthesized. In addition, their physical properties and enzyme activity were investigated.

2. Materials and Methods

All the reagents and solvents were purchased from commercial sources. Astuart digital SMP30 melting point device was used to measure melting points. A Shimadzu FT−IR model 4800S spectrophotometer was used to record FT−IR spectra over the range 4000−400 cm^{-1}. A Shimadzu recorded UV-Visible spectra 160 by using a quartz cell 1 cm and measured at (200-1100) nm in dimethyl sulfoxide (DMSO) at 25C°. Atomic absorption was measured using a Shimadzu AA 680 G. Elemental analysis (CHN) of the ligand (L´) and calibration-type linear regression EA were performed on its metal complexes. The ^{1}H-NMR and ^{13}C-NMR of the ligand (L´) was registered at a spectrophotometer Bruker DMx-500 (300 MHz) by using DMSO− d_6 and $(CD_3)_2CO$. The magnetic susceptibility of the synthesized complexes was determined by using an automatic magnetic susceptibility balance at room temperature (RT) in Inolab Multi 740, 82362 WTW, which was also used to measure the conductivity of solutions in DMSO solvent.

2.1. Synthesis of the ligand (L´)

The new Schiff base ligand (L´) was prepared by condensing a solution of (0.137 g, 0.001 mol) isoniazid (isonicotinohydrazide) in 10 mL of absolute ethanol. Gradually, this solution was added to an acidified mixture containing glacial acetic acid drops and 0.182 g (0.001 mol) of 4-hydroxy-3,5-dimethoxybenzaldehyde, dissolved in 10 mL of absolute ethanol. The final reaction mixture was refluxed for 8 hrs. The resulting yellow precipitate was filtered, washed with absolute ethanol, dried at room temperature, and finally recrystallized from hot absolute ethanol. The synthesized ligand (L´) was tested for solubility in ethanol, methanol, chloroform, tetrachloroethane, dimethylformamide, and DMSO. The purity of the ligand (L´) was determined by TLC on silica gel as the stationary phase and (Hexane/Ethyl acetate) as the washing solvent in a specific ratio, with a melting point of 71% (228−230)°C. The preparation reaction of the ligand (L´) is illustrated in **Scheme 1**.

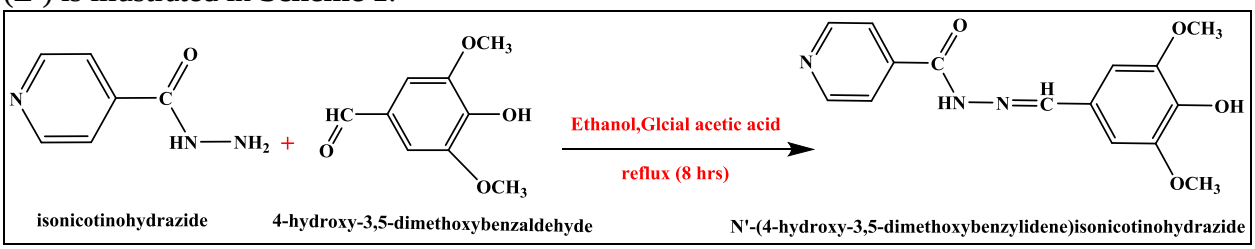

Scheme 1. Synthesis of N'-(4-hydroxy-3,5-dimethoxybenzylidene) isonicotinohydrazide Schiff base ligand

2.2. Preparation of metal complexes

The complexes were prepared by adding a two-fold excess of ligand (L´) solution to one mole of an ethanoic metal salt solution. The salts of [$CoCl_2$. $6H_2O$ (0.238 g, 1.00 mmol)], [$NiCl_2$. $6H_2O$ (0.238 g, 1.00 mmol)], [$CuCl_2$. $2H_2O$ (0.169 g, 1.00 mmol)], and [$PdCl_2$ (0.177 g, 1.00 mmol)] were added to 0.602 g (2.00 mmol) of the ligand (L´). A color change was observed after mixing the two solutions. The reaction mixture was then heated under reflux for 8 hrs. The resultant was filtered through filter paper, washed with ethanol, and then air-dried at room temperature.

3. Results

3.1. General physical characterization for the ligand (L´) and its complexes

The physical properties, including color, melting point, yield %, and metal analysis of the ligand (L´) and its complexes, were illustrated in **Table 1,** and solubility in **Table 2**.

Table 1. General physical characterization of the ligand (L´) and complexes

Molecular Formula of compound	M wt. g/mol	Melting point °C or dec.	Color	Yield %	Elemental micro analysis (calc.)%				
					C	H	N	M	Cl
$C_{15}H_{15}N_3O_4$ (L)	301.17	228-230	Yellow	71	59.31 (59.71)	4.78 (4.98)	13.88 (13.94)	-	-
$[Co(L')_2Cl_2]$ $C_{30}H_{30}N_6O_8Cl_2Co$	732	234-236	Green	63	49.11 (49.18)	4.05 (4.09)	11.39 (11.47)	8.05 (8.06)	9.65 (9.69)
$[Ni(L')_2Cl_2]$ $C_{30}H_{30}N_6O_8Cl_2Ni$	732.1	245-247	Brown	54	49.20 (49.18)	4.10 (4.09)	11.40 (11.47)	8.09 (8.06)	9.63 (9.69)
$[Cu(L')_2]Cl_2$ $C_{30}H_{30}N_6O_8Cl_2Cu$	736.6	Dec.226	Brown	79	48.83 (48.87)	4.03 (4.07)	11.39 (11.40)	8.54 (8.62)	9.60 (9.63)
$[Pd(L')_2]Cl_2$ $C_{30}H_{30}N_6O_8Cl_2Pd$	779.4	252-254	Dark	81	46.15 (46.17)	3.86 (3.84)	10.76 (10.77)	13.60 (13.65)	9.12 (9.10)

*Calc. =calculated, Dec.= decomposition temperature.

Table 2. The solubility of ligand (L´) and its complexes in various solvents

Complexes	H_2O	EtOH	MeOH	THF	Acetone	$CHCl_3$	DMF	DMSO
$C_{15}H_{15}N_3O_4$ (L´)	—	+	+	+	—	+	+	+
$[Co(L')_2Cl_2]$	—	÷	÷	—	+	—	+	+
$[Ni(L')_2Cl_2]$	—	÷	÷	—	+	—	+	+
$[Cu(L')_2]Cl_2$	—	÷	÷	—	+	—	+	+
$[Pd(L')_2]Cl_2$	—	÷	÷	—	+	—	+	+

*Where: (+) = soluble, (—) = insoluble and, (÷) = partially soluble.

3.2. ^{1}H-Nuclear magnetic resonance spectrum for the (L´) ligand

The chemical shifts for the ligand (L´) are shown in **Figure 1**.

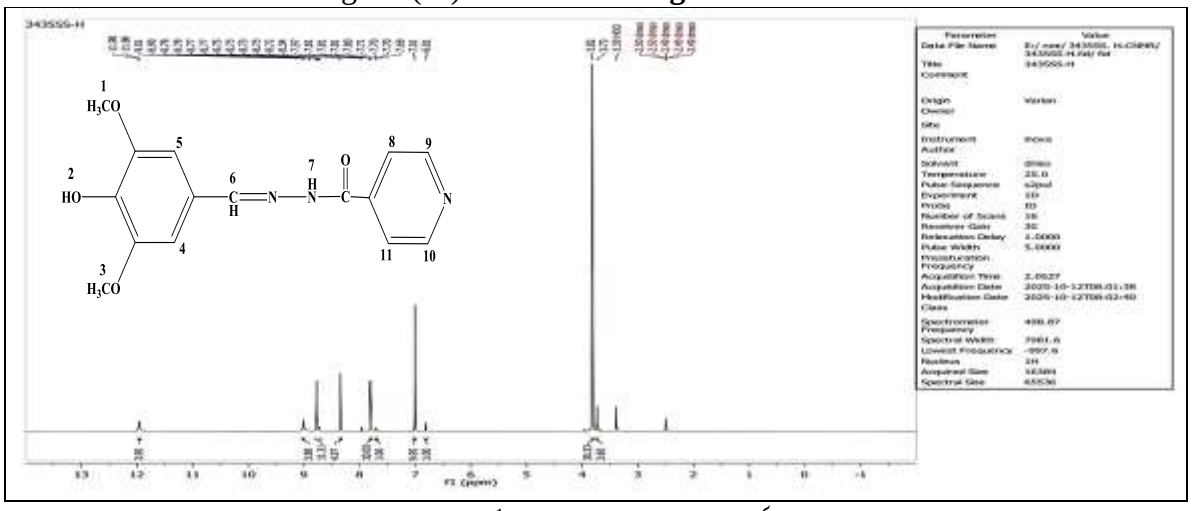

Figure 1. The ^{1}H–NMR spectrum of (L´) ligand

3.3. ^{13}C-Nuclear magnetic resonance spectrum for the (L´) ligand

Figure 2 shows the chemical shift of the ligand (L´).

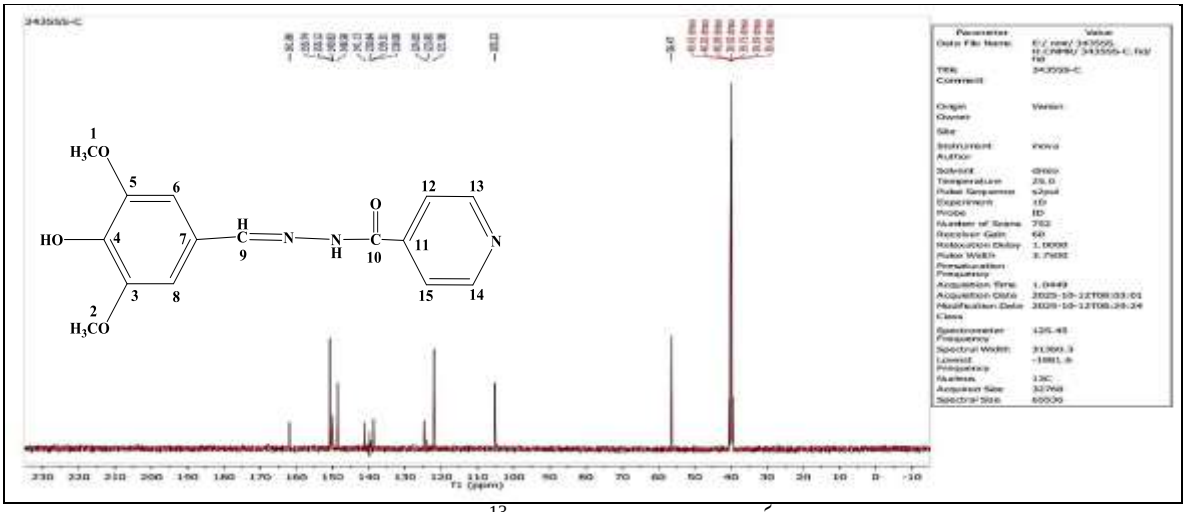

Figure 2. The ^{13}C–NMR spectrum of (L´) ligand

3.4. Fourier transform infrared spectroscopy of the ligand (L´) and its complexes

The IR bands of the ligand (L´) and its complexes were illustrated in **Table 3**; **Figure 3** shows FT-IR for (L´), and **Figure 4** shows FT-IR of [Co (L´)$_2$Cl$_2$].

Table 3. Infrared spectra for the ligand (L´) and its complexes

Compounds	υ (N-H) δ (N-H) cm^{-1}	υ (C=O) cm^{-1}	υ (C=N) cm^{-1}	υ (N-N) cm^{-1}	υ (M-N) cm^{-1}	υ (M-O) cm^{-1}	υ (C=C) Ar. cm^{-1} υ (C-H) Ar. cm^{-1} υ (C-H) Aliph. cm^{-1}
$C_{15}H_{15}N_3O_4$ (L´)	3178 (br)	1649 (s)	1581(s)	1060 (s)	___	___	1510 (s) 3072 (br) 2967 (br), 2848 (br)
[Co (L´)$_2$Cl$_2$]	3244 (s) 1538 (s)	1610 (s)	1588 (s)	1066 (m)	558 (s)	480 (s)	1515 (s) 3070 (m) 2960 (w), 2840 (w)
[Ni (L´)$_2$Cl$_2$]	3428 (br) 1546 (s)	1658 (s)	1588 (s)	1066 (s)	581(m)	476 (m)	1528 (m) 3060 (m) 2981 (s) , 2902 (s)
[Cu (L´)$_2$]Cl$_2$	3377 (m) 1549 (m)	1617 (m)	1585 (s)	1060 (sh)	546 (br)	499 (br)	1549 (m) 3067 (m) 2966 (m),2872(m)
[Pd (L´)$_2$] Cl$_2$	3346 (br) 1577 (s)	1655 (br)	1614(s)	1041 (s)	585 (br)	480 (br)	1531 (s) 3050 (sh) 2976 (br), 2860 (br)

br.= broad, m.= medium, s.= strong, sh.= sharp, w.= weak.

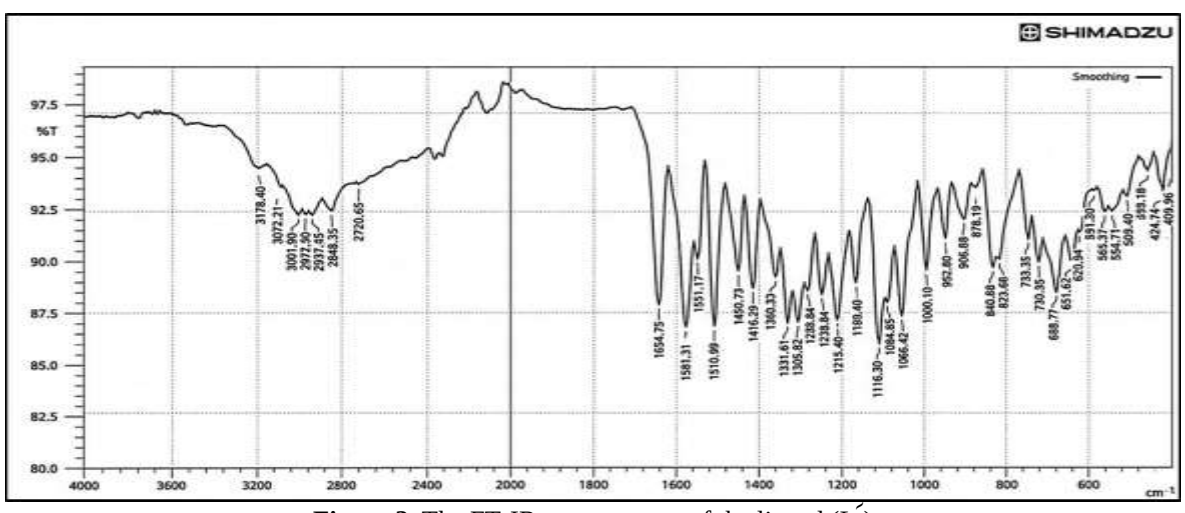

Figure 3. The FT-IR spectroscopy of the ligand (L´)

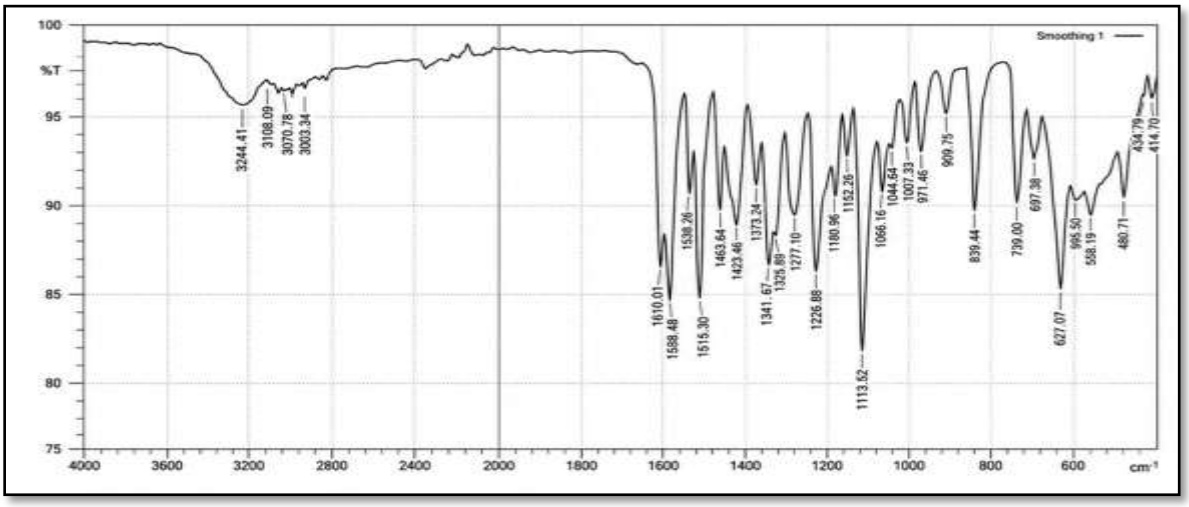

Figure 4. The FT-IR spectroscopy of [Co (L´)$_2$Cl$_2$]

3.5. Electronic spectrum and magnetic properties for the ligand (L´) and its complexes

The ultraviolet-visible spectrum of (L´), the ligand, and its prepared complexes resolved in DMSO (10^{-3} mole/L) were measured, and the values of μeff, the effective magnetic moment at (300 K) room temperature, and the electronic spectrum of the ligand (L´) and complexes recorded in DMSO solution at wavelengths (200-800) nm were determined. Their data are listed in **Table 4**.

Table 4. Electronic spectral data, magnetic moment, molar conductance, and the proposed geometry for the ligand (L´) and complexes

Compound	λ nm	ύ cm^{-1}	ε max ($mol^1.L.cm^1$)	The electronic Transitions	ΛM (DMSO) S. cm^2. mol^{-1}	μ_{eff} (B.M) Suggested geometry
$C_{15}H_{15}N_3O_4$ (L´)	251 363	39840 27548	1885 111	$\pi \rightarrow \pi^*$ n$\rightarrow \pi^*$	———	———
[Co (L´)$_2$Cl$_2$]	340 483	29411 20703	1284 747	C.T $^4T_1g_{(F)} \rightarrow {}^4T_1g_{(P)}$	9.43	4.80 Octahedral
[Ni (L´)$_2$Cl$_2$]	284 352 430	35211 28409 23255	1022 198 160	$\pi \rightarrow \pi^*$ C.T $^3A_2g_{(F)} \rightarrow {}^3T_1g_{(P)}$	10.12	2.38 Octahedral
[Cu (L´)$_2$]Cl$_2$	345 470	28985 21276	498 475	C.T $^2B_1g \rightarrow {}^2Eg$	74.51	1.65 Square planer
[Pd (L´)$_2$] Cl$_2$	339 492	29498 20325	641 660	C.T $^1A_1g \rightarrow {}^1B_1g$	78.30	Diamagnetic Square planer

3.6. Molar conductance for the prepared complexes

The suggested structures for the prepared complexes are illustrated in **Figure 5.**

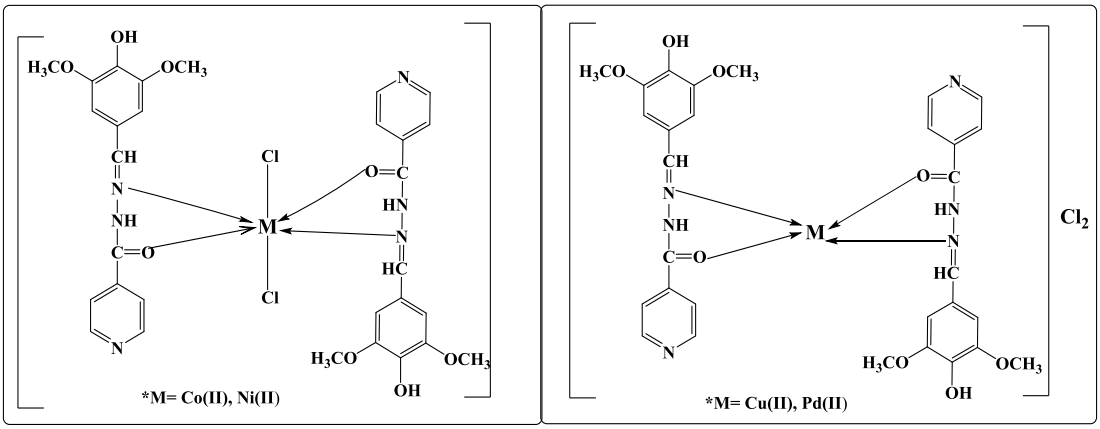

Figure 5. The proposed structures for the prepared complexes

3.7. Study of complexes' formation in solution mole ratios

Figure 6 illustrates the mole-ratio slope for [Co (L´)$_2$Cl$_2$], and **Figure 7** represents the molar-ratio slope for [Ni (L´)$_2$Cl$_2$].

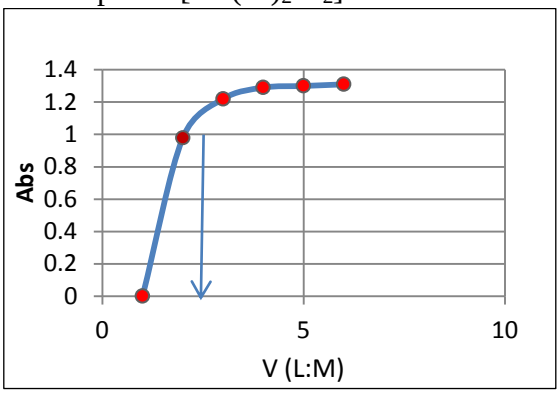

V (L:M)	Abs
0.5:1	0.26
1:1	0.98
2:1	1.22
3:1	1.29
4:1	1.3
5:1	1.31

Figure 6. The mole- ratio slop for [Co (L´)$_2$Cl$_2$]

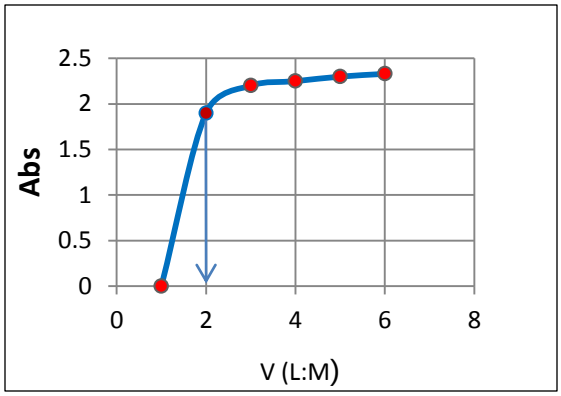

V (L:M)	Abs
0.5:1	0.60
1:1	1.9
2:1	2.2
3:1	2.25
4:1	2.3
5:1	2.33

Figure 7. The mole- ratio slop for [Ni (L´)$_2$Cl$_2$]

3.8. Studying of enzyme activity methods: Determination of AST activity

The colorimetric approach was used to assess AST activity in human serum. The ligand's biological activity and its metal complexes, as well as the inhibition percentages, were determined by comparing activity in the presence and absence of inhibition under identical conditions, according to the following equation; **Table 5** presents them.

$$\%\,\text{inhibition} = 100 - \frac{\text{the activity in the presences of inhibitor}}{\text{the activity in the absence of inhibitor}} * 100 \qquad \textbf{(1)}$$

Table 5. The effect of the varying of the ligand (L´) and complex concentrations on human serum (AST)

Compound	Inhibition concentration (M)	AST Activity (IU/L)	Inhibition %
Control	zero	360	—
$C_{15}H_{15}N_3O_4$ (L´)	10^{-2}	260	27.8
	10^{-4}	275	23.6
	10^{-6}	300	16.7
	10^{-8}	335	6.9
[Co (L´)$_2$Cl$_2$]	10^{-2}	310	13.9
	10^{-4}	335	7
	10^{-6}	360	0
	10^{-8}	360	0
[Ni (L´)$_2$Cl$_2$]	10^{-2}	349	13.0
	10^{-4}	330	8.4
	10^{-6}	360	0
	10^{-8}	360	0
[Cu (L´)$_2$]Cl$_2$	10^{-2}	65	82.0
	10^{-4}	200	44.4
	10^{-6}	310	13.8
	10^{-8}	333	7.5
[Pd (L´)$_2$] Cl$_2$	10^{-2}	66	81.7
	10^{-4}	135	62.5
	10^{-6}	200	44.4
	10^{-8}	340	5.5

3.9. The antimicrobial study

The zones of inhibition of fungal and bacterial activity around the samples are shown in **Table 6**.

Table 6. The effect of the prepared ligand (L´) and its complexes against fungus and G^- and G^+ bacteria

Compounds	Inhibition zone (mm) diameter at concentration 10^{-3}				
	Candida albicans	G- bacteria		G+ bacteria	
		E.coli	*pseudomonas aeruginosa*	*Staphylococcus aureus*	*Enterococcus Spp*
Amoxicillin	25.4	26	23.4	27.2	28.6
$C_{15}H_{15}N_3O_4$ (L´)	0	0	14	0	12
[Co (L´)$_2$Cl$_2$]	12	0	0	12	13
[Ni (L´)$_2$Cl$_2$]	12	0	12	13	11
[Cu (L´)$_2$]Cl$_2$	0	0	14	14	14
[Pd (L´)$_2$] Cl$_2$	25	13	12	0	12

4. Discussion

4.1. The ^{1}H-Nuclear magnetic resonance spectrum for the (L´) ligand

The ^{1}H-NMR spectrum of the ligand (L´) showed a signal at δ H= 11.96 ppm due to the phenolic (O-H) proton[11]. The chemical shift at δ H = 9.01 ppm indicates the azomethine proton[12]. The spectrum shows signals for the protons of the aromatic rings at δ H= 7.69–8.78 ppm. A signal at δ H= 7.01 ppm is equivalent to the proton assigned to the (NH) group[13]. The singlet signals at δH= 3.73-3.82 ppm belong to the (OCH_3) group[14]. The spectrum

4.2. The ^{13}C-Nuclear magnetic resonance spectrum for the (L´) ligand

The ^{13}C-NMR for ligand (L´) in DMSO-d6 revealed the chemical shift in the range (δ= 161.86 ppm) assigned to the carbon of the carbonyl group (C=O) (C_{10})[15]. The chemical shift of the carbon atom of azomethine is (δ=150.74 ppm) (C_9)[16]. The chemical shift appeared at (150.12 ppm, 149.83 ppm) (C_3, C_5) due to (C─OCH_3). The chemical shift in the range (δ 148.58 ppm) is due to (C─OH) (C_4); the chemical shifts in the range (δ 105.23-δ 141.13) ppm are attributed to carbon atoms of the aromatic ring. The chemical shift at (δ=56.47 ppm) is assigned to the (─OCH_3) group (C_1, C_2). The signal at 39.42-40.42 ppm is due to the solvent.

4.3. FT- IR spectrum for the ligand (L´) and its complexes

The IR spectrum of ligand (L´) showed a band at (3178) cm-^{1}, corresponding to the υ(N-H) frequency. The strong band observed at (1649) cm-1 is due to the (C=O) group of INH (isoniazid)[17]. The band at υ (1581) cm^{-1} is assigned to the azomethine (C=N) stretching frequency of the ligand (L´). The observed bands at (1510) cm^{-1} and (3072) cm^{-1} are assigned to the aromatic (C=C) and (C-H) stretching frequencies, respectively[18]. υ(C=N) for the Schiff base's vibration frequency was shifted to higher or lower frequencies in the complexes. The vibration stretching of the ligand (L´) donated υ (C=O) exhibited a frequency shift to either a higher or lower frequency in the range (1610-1658) cm^{-1} in the spectra of the complexes[19]. IR spectra of all complexes showed new bands in the range (546-585) cm^{-1} and (476-499) cm^{-1}, which were assigned to υ (M-N) and υ (M-O), respectively[20].

4.4. Electronic spectrum and magnetic properties of the ligand (L´) and complexes

Electronic spectrum data and magnetic susceptibility measurements were used to determine the composition of the complexes. UV- visible spectra of the yellow solution for the synthesized (L´) ligand showed a pair of peaks at (251 nm, 39411 cm^{-1}) and (363 nm, 27548 cm^{-1}), which may be assigned to the ($\pi \rightarrow \pi^*$), ($n \rightarrow \pi^*$)[21]. These electronic transitions shifted to higher or lower frequencies in the electronic spectra of all complexes produced, confirming ligand coordination to the metals. Absorption peaks at (340 nm, 29411 cm^{-1}), (352 nm, 28409 cm^{-1}), (345 nm, 28985 cm^{-1}), and (339 nm, 29498 cm^{-1}) were assigned to charge transfer (C.T.) for [Co (II), Ni (II), Cu(II), and Pd(II)] complexes, respectively. The peak of Co (II) observed at 340 nm (29411 cm^{-1}) was assigned to the field transition of the ligand, and the peak at 483nm (20703 cm^{-1}) was

due to (^4T_1g (F) → ^4T_1g (P)). The computed effective magnetic moment value was 4.80 B.M., within the limits for the predicted octahedral geometry range of [22]. The Ni (II) spectrum showed one peak at 430 nm (23255 cm^{-1}) attributed to (^3A_2g (F) →^3T_1g (P))[23]. The magnetic moment was 2.38 B.M.; the ligand-field characteristics indicated an octahedral structure around Ni(II). The Cu(II) spectrum showed a peak at 470 nm (21276 cm^{-1}), corresponding to the transition (^2B_1g → ^2Eg). This peak position is consistent with square-planar geometry, and the magnetic moment value is 1.65 B.M.[24]. The UV-visible spectrum of the Pd(II) complex exhibited a new absorption peak at 492 nm (20325 cm^{-1}) due to (^1A_1g→ ^1B_1g). The Pd(II) complex was square planar due to ^{4} *d*-systems. The magnetic moment of the Pd complex was confirmed to be diamagnetic[25].

4.5. Molar conductance for prepared complexes

The low molar conductivity values for Co(II) and Ni(II) complexes (9.43 and 10.12 $S.cm^2.mol^{-1}$) in DMSO indicate non-electrolytic behavior and the formulation $[M(L)_2Cl_2]$. Whereas the Cu(II) and Pd(II) complexes have higher molar conductivities (74.51 and 78.30 $S.cm^2.mol^{-1}$), indicating electrolytic behavior and supporting the formulation $[M(L)_2]Cl_2$, with chloride ions present in solution[26].

4. 6. Study of complex formation in solution: The molar-ratio method

The molar ratio method is used to determine the ratio of metal ions to ligand [L:M] in the complex solution. Ethanol was used as a solvent in this study. A series of solutions containing a fixed amount of metal and different ligand concentrations (2×10^{-3} M) was prepared. The absorbance was measured at (λ_{Max}) for the complex. The relationship between the absorbance and the ratio of [L] / [M] was drawn to determine the L/M and the results ($2x10^{-3}$ M) where the metal fixed and the ligand concentration changed in the presence of an ethanoic solution. A plot would show absorbance increasing with ligand addition until the [L]/[M] ratio reaches 2. This indicates a [2:1] stoichiometry for both Co(II) and Ni(II)[27].

4.7. The antimicrobial study

The biological activity of the synthesized ligand (L´) and its complexes was tested against chosen species of microorganisms, including the G+ bacteria (such as *Enterococcus spp*. and *Staphylococcus aureus*) and the G- bacteria (such as *Pseudomonas aeruginosa* and *E. coli*)[28], and antifungal activity (*Candida albicans*) in agar[29]. Samples were dissolved in DMSO to provide a final concentration of 10^{-3} mg/mL. The dissolved samples were used to determine the area of inhibition of microbial growth on the agar plates. Agar plates were incubated for 24 hours at 37 °C. The investigation showed that Cu (II) exhibited good activity against *Enterococcus*, *Staphylococcus aureus*, and *Pseudomonas aeruginosa*. Pd (II) complexes displayed significant antimicrobial potential, with superior antifungal activity against *Candida albicans* and good activity against *E. coli*, *Enterococcus*, and *Pseudomonas aeruginosa* compared to the free ligand and other complexes. This may be due to improved fungal cell permeability, confirming preferential antifungal efficacy alongside moderate antibacterial performance.

5. Conclusion

This study demonstrated that condensation of isonicotinohydrazide with 4-hydroxy-3,5-dimethoxybenzaldehyde yields a new bidentate ligand with potential metal-ion binding sites. The Schiff base coordinates through the azomethine nitrogen and oxygen atoms, acting as a bidentate ligand. Various geometric shapes are achieved by coordinating the synthesized ligand with specific bivalent metal ions. Spectroscopic analysis showed that metal ions coordinate through (N-O) donor atoms. These include the nitrogen atom of the imine group and the oxygen atom of the carbonyl group. The analysis suggested that the Co(II) and Ni(II) complexes possess an octahedral geometry. They are coordinated to the (O, N) atoms of the ligand in a bidentate mode. In contrast, Cu(II) and Pd(II) adopt a square-planar geometry. For the enzyme-activity study, DMSO was used to denote the inhibitory effects; the inhibitory concentration was 10^{-2} M for

Co(II), Ni(II), Cu(II), and Pd(II). The resulting compound, used as an antibacterial against four bacterial species (both G+ and G-), demonstrated good efficacy with $[Pd(L')_2]Cl_2$.

Acknowledgment

The authors thank the Department of Chemistry, College of Education for Pure Science (Ibn Al-Haitham), University of Baghdad, Baghdad, Iraq, for providing the resources needed for this research project.

Conflict of Interest

The authors declare that they have no conflicts of interest.

Funding

This research did not receive external funding.

References

1. Subasi NT. A comprehensive review on schiff bases: Development process, green synthetic strategies, and versatile applications. In: Subasi NT, editor. Schiff bases-Recent developments and application areas. London: IntechOpen; 2025. p. 238. https://doi.org/10.5772/intechopen.1012219.
2. Gomathi GV, Rajaram R, Kayathri Devi K, Gayathri M, Ishwarya PP, Jagatheeshwari P, Karthika R, Keerthana D. Synthesis, spectral investigation and antimicrobial assay of 2-ethoxy-6-(((3-nitrophenyl)imino)methyl)phenol and its Co(II) and Cu(II) complexes. Discov Chem. 2025;2(1):1-13. https://doi.org/10.1007/s44371-025-00185-0.
3. Khan Z. Schiff bases and their transition metal complexes : A review on biological facets. Med Chem (Los Angeles). 2022;12(7):1–10. https://doi.org/10.37421/2161-0444.2022.12.630.
4. Li Y, Yang ZS, Zhang H, Cao BJ, Wang FD, Zhang Y, Shi YL, Yang JD, Wu BA. Artemisinin derivatives bearing Mannich base group: synthesis and antimalarial activity. Bioorg Med Chem. 2003; 11(20):4363-4368. https://doi.org/10.1016/S0968-0896(03)00499-1.
5. Abu-Yamin AA, Abduh MS, Saghir SAM, Al-Gabri N. Synthesis, characterization and biological activities of new schiff base compound and its lanthanide complexes. Pharmaceuticals (Basel). 2022;15(4): 454. https://doi.org/10.3390/ph15040454.
6. Abdallah SM, Mohamed GG, Zayed MA, Abou El-Ela MS. Spectroscopic study of molecular structures of novel Schiff base derived from o-phthaldehyde and 2-aminophenol and its coordination compounds together with their biological activity. Spectrochimica Acta Part A: Molecular and Biomolecular Spectroscopy.2009;73(5):833-840. https://www.sciencedirect.com/science/article/pii/S1386142509001620.
7. Pallikkavil R, Ummathur MB, Krishnankutty K. Schiff bases of terephthalaldehyde with 2-aminophenol and 2-aminothiophenol and their metal complexes. Sch Res Libr Arch. 2012;4(5): 2223–2227.
8. Raji Sankar, T.M. Sharmila. Schiff bases-based metallo complexes and their crucial role in the realm of pharmacology. Results in Chemistry. 2023;6(2211-7156):101179. https://doi.org/10.1016/j.rechem.2023.101179.
9. Mushtaq I, Ahmad M, Saleem M, Ahmed A. Pharmaceutical significance of schiff bases : an overview. Futur J Pharm Sci. 2024;10(16):1-12. https://doi.org/10.1186/s43094-024-00594-5.
10. Awolope RO, Ejidike IP, Clayton HS. Schiff base metal complexes as a dual antioxidant and antimicrobial agents. J Appl Pharm Sci. 2023;13(3):132–140. https://dx.doi.org/10.7324/JAPS.2023.91056.
11. Charisiadis P, Kontogianni VG, Tsiafoulis CG, Tzakos AG, Siskos M, Gerothanassis IP. ^{1}H-NMR as a structural and analytical tool of intra- and intermolecular hydrogen bonds of phenol-containing natural products and model compounds. Molecules. 2014;19(9):13643-13682. https://doi.org/10.3390/molecules190913643.
12. Preethi B, Sathiyaseelan M, Prabakaran K, Kutti Rani S, Sivashanmugam G, Srinivasan AP. Theoretical and spectral investigation of some schiff bases. Der Pharma Chem. 2018;10(11):88–96.
13. Faria CF, Moreira T, Lopes P, Costa H, Krewall JR, Barton CM, Santos S, Goodwin D, Machado D, Viveiros M, Machuqueiro M, Martins F. Designing new antitubercular isoniazid derivatives with

improved reactivity and membrane trafficking abilities. Biomed Pharmacother [Internet]. 2021;144:112362. https://doi.org/10.1016/j.biopha.2021.112362.

14. Safronov NE, Kostova IP, Palafox MA, Belskaya NP. Combined NMR spectroscopy and quantum-chemical calculations in fluorescent 1,2,3-triazole-4-carboxylic acids fine structures analysis. Int J Mol Sci. 2023;24(10):8947. https://doi.org/10.3390/ijms24108947.
15. Saleh HA, Alkhatib AS, Abdul Rahman, Al-Jeboori MJ. Synthesis, structural characterisation and biological evaluation of new semicarbazone metal complexes derived from Mannich-base. Biochem Cell Arch. 2021;21(1):159-168. https://connectjournals.com/03896.2021.21.159.
16. Sambasevam KP, Mohamad S, Sarih NM, Ismail NA. Synthesis and characterization of the inclusion complex of β-cyclodextrin and azomethine. Int J Mol Sci. 2013;14(2):3671-82. https://www.mdpi.com/1422-0067/14/2/3671
17. Poggi M, Barroso R, Costa-Filho AJ, de Barros HB, Pavan F, Leite CQ, Gambino D, Torre MH. New isoniazid complexes, promising agents against mycobacterium tuberculosis. J Mex Chem Soc. 2013;57(3): 198–204. https://doi.org/10.29356/jmcs.v57i3.207.
18. Kindness A, McKean DC, Stewart D. Infrared intensities of CH stretching bands in partially deuterated compounds, and effects of conformation and substitution J Mol Struct. 1990;224:363–384. https://doi.org/10.1016/0022-2860(90)87030-2.
19. Mahmoud WA, Hassan ZM. Synthesis and spectral analysis of some metal ions complexes withmixed ligands of schiff base and 1,10-phenanthroline synthesis and spectral analysis of some metal ions complexes with mixed ligands of schiff base and 1,10-phenanthroline. Baghdad Sci J. 2017;14(1):135-145. https://doi.org/10.21123/bsj.2017.14.1.0135.
20. Nakamoto K. Infrared and raman spectra of inorganic and coordination compounds. 6th ed. New Jersey: John Wiley & Sons, Ltd ; 2009. https://doi.org/10.1002/0470027320.s4104.
21. Vinusha HM, Kollur SP, Revanasiddappa HD, Ramu R, Shirahatti PS, Prasad MNN, Chandrashekar S, Begum M. Preparation, spectral characterization and biological applications of Schiff base ligand and its transition metal complexes. Results Chem. 2019; 1:100012. https://doi.org/10.1016/j.rechem.2019.100012.
22. Hadi MA, Kareem IK, Atban AK. Synthesis and characterization of novel metal complexes with new Schiff base ligand derived from 6-amino pencillic acid and toxicological studies of its complex with Au(III) on human cells for colon cancer LS-174. Biochem Cell Arch. 2021;21(1):2477–2488. https://connectjournals.com/03896.2021.21.2477.
23. Rajn k. Synthesis and studies on electronic spectra of Ni (II) complexes with 3-hydroxy-2-naphthalidene semicarbazone. Int J Sci Dev Res. 2020;5(3):177–180. https://ijsdr.org/papers/IJSDR2003034.pdf.
24. Lomjanský D, Rajnák C, Titiš J, Moncoľ J, Smolko L, Boča R. Impact of tetrahedral and square planar geometry of Ni(II) complexes with (pseudo)halide ligands to magnetic properties. Inorganica Chim Acta. 2018;483:352–358. https://doi.org/10.1016/j.ica.2018.08.029.
25. Lupașcu G, Pahonțu E, Shova S, Bărbuceanu SF, Ilieș DC, Badea M, Paraschivescu C, Ducu C, Neamțu J, Dinu M, Ancuceanu RV, Drăgănescu D, Dinu-Pîrvu CE. Synthesis, characterization, crystal structure and toxicity evaluation of Co (II), Cu (II), Mn (II), Ni (II), Pd (II) and Pt (II) complexes with Schiff base derived from 2-chloro-5-(trifluoromethyl)aniline. Appl Organomet Chem. 2020;34:e5931. https://doi.org/10.1002/aoc.5931.
26. BekeleY, Achalu C, Thillai A. Synthesis and characterization of Co (II) and Ni (II) complexes of Schiff base derived from ninhydrin and valine. Int J chemtech Res. 2020;13(03):265–273. https://www.sphinxsai.com/2020/ch_vol13_no3/3/(265-273)V13N3CT.pdf
27. Mabrouk M, Hammad SF, Abdelaziz MA, Mansour FR. Ligand exchange method for determination of mole ratios of relatively weak metal complexes: A comparative study. Chem Cent J. 2018;12(1):143. https://doi.org/10.1186/s13065-018-0512-4.
28. Tavares TD, Antunes JC, Padrão J, Ribeiro AI, Zille A, Amorim MTP, Ferreira F, Felgueiras HP. Activity of specialized biomolecules against Gram-positive and Gram-negative bacteria. Antibiotics (Basel). 2020;9(6):314. https://doi.org/10.3390/antibiotics9060314.
29. Macias-Paz IU, Pérez-Hernández S, Tavera-Tapia A, Luna-Arias JP, Guerra-Cárdenas JE, Reyna-Beltrán E. Candida albicans the main opportunistic pathogenic fungus in humans. Rev Argent Microbiol. 2023;55(2):189-198. https://doi.org/10.1016/j.ram.2022.08.003.